

SOLUTION STRUCTURE OF BRANCHED $U_3'p_5'A_2'p_5'G$ AND ITS COMPARISON WITH $A_2'p_5'G$ BY 500 MHz NMR SPECTROSCOPY

C. Glemarec, M. Jaseja, A. Sandström, L. Koole, P. Agback and J. Chattopadhyaya*

Department of Bioorganic Chemistry, Box 581, Biomedical Center,
University of Uppsala, S-751 23 Uppsala, Sweden

(Received in UK 12 November 1990)

Summary: In this study, the 1H - 1H , 1H - ^{31}P and ^{13}C - ^{31}P coupling constants of the branched RNA tetramer 2 have been measured at two temperatures to obtain detailed information about its backbone conformation. Evaluation of these coupling constants by Karplus-Altona algorithm shows the decrease of populations of γ^+ and β^1 upon temperature-increase for the branch-point A and 3'-terminal C residues, which have been attributed to a destacking along the $U_3' \rightarrow 5'A_3' \rightarrow 5'C$ stacked axis in the tetramer 2. In accordance with this observation, it has been clearly established that γ^+ and β^1 populations of constituent $2' \rightarrow 5'$ -linked guanosine nucleotide is rather insensitive to temperature-change. The NOEs seen at 270 MHz between AH8 with UH6, and AH2 with CH6 also support that the tetramer 2 stacks along the $U_3' \rightarrow 5'A_3' \rightarrow 5'C$ axis. The NOEs observed at 270 MHz between CH6 with GH8, and UH6 with GH8 suggest also a spatial proximity between 5'-terminal U and 2'-terminal G, and 3'-terminal C and 2'-terminal G residues. These observations have led us to propose a two-state model for the tetramer 2. On the other hand, detailed temperature-dependent measurements of 1H - 1H , 1H - ^{31}P and ^{13}C - ^{31}P coupling constants and chemical shifts of analogues of the branched trimer 1 in this laboratory and elsewhere have shown that the molecular conformation of the branched trimer 1 is governed by $A_2' \rightarrow 5'G$ stack. The introduction of a 5'-terminal uridine residue in trimer 1 to tetramer 2 shifts the molecular conformation from an $A_2' \rightarrow 5'G$ stack in the trimer 1 to a $A_3' \rightarrow 5'C$ stack in the tetramer 2. This is a new example of 5'-terminal residue promoted conformational transmission.

In group II splicing of RNA precursors, a lariat RNA is formed at the penultimate step of ligation of exons. In the final step of splicing, this lariat is excised upon the Mg^{2+} promoted ligation of two exons. The nucleotide sequence at the branch site in the lariat is highly conserved¹. In the lariat formed, the branch-point is always an adenosine residue which is linked through its 2'-phosphate to the 5'-hydroxy group of a guanosine nucleotide, and through its 3'-phosphate to the 5'-hydroxy group of a pyrimidine nucleotide. In the group II splicing reaction, the lariat formed always carries a uridine residue next to the 5'-end of the branch point adenosine while in the Nuclear pre-messenger RNA splicing reaction, it is always an adenosine nucleotide. Mutation experiments have shown that replacement of the branch point adenosine by guanosine, uridine or cytidine either stops the splicing reaction, or promotes wrong splicing in the upstream region of the pre-mRNA². It has also been shown that guanosine as the $2' \rightarrow 5'$ linked nucleotide is necessary for the completion of the second step of the splicing reaction. In last few years, we have been trying to understand the structural significance of formation of branch-RNA in the splicing reaction, and the structural and conformational basis for the choice of adenosine as the branch-point nucleotide and of guanosine as the $2' \rightarrow 5'$ linked nucleotide.

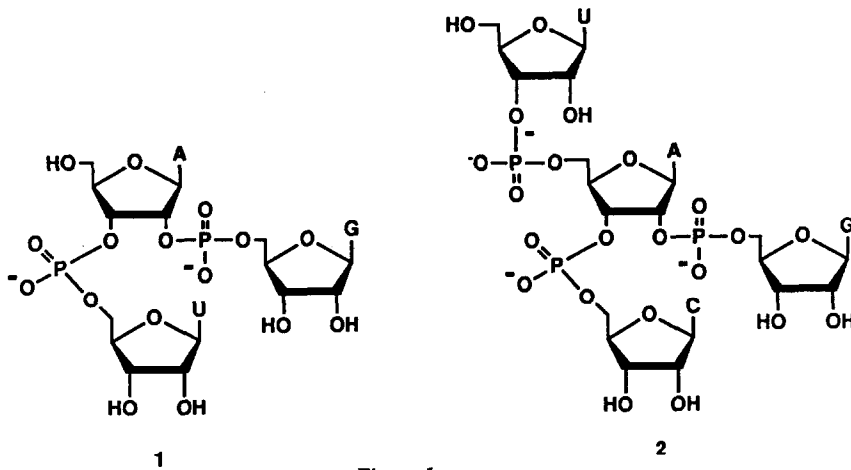


Figure 1

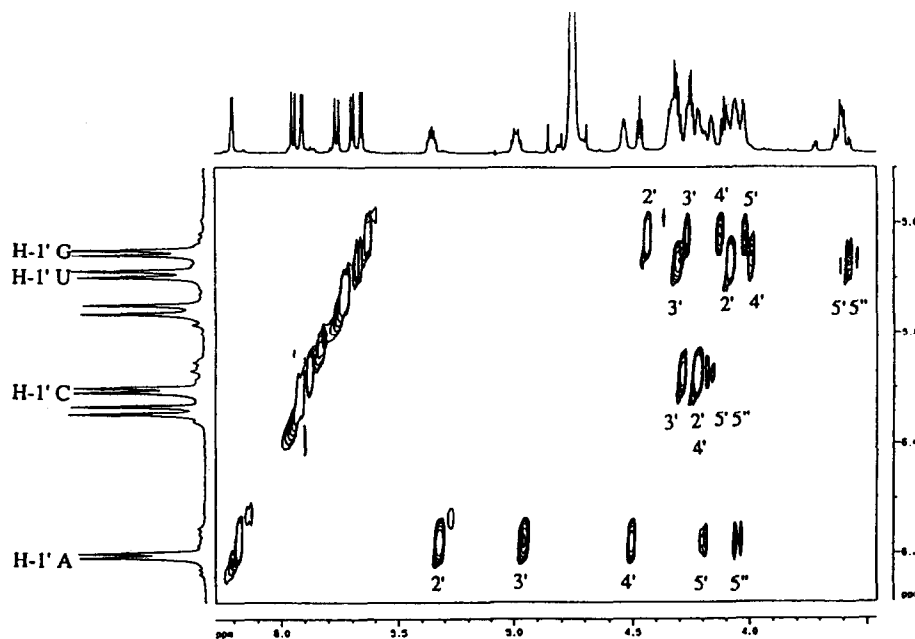


Figure 2: Homonuclear Hartmann-Hahn spectrum for 2 at 27 °C in D₂O. The direct connectivities for each sugar residue are indicated. The fact that the 5' and 5'' protons of the 2'-guanosine residue are superimposed while the 5' and 5'' protons of the adenosine, cytosine and uridine are separated is an indication that the guanosine residue does not participate in any strong stacking in the molecule.

As an attempt to answer these questions, we³ and others^{4,5} have studied the conformational properties by ¹H, ³¹P-NMR and CD spectroscopy of several trimeric branched RNA fragments and have come to the conclusion that their structures are dominated by A2'→5'G stack. Our laboratory has subsequently shown through a preliminary 270 MHz NMR study on branched tetramers, based on NOE and temperature-dependent chemical shifts, that their conformational features were mainly comprised of A3'→5'Py stack⁶. In this paper, we wish to report our detailed ¹H, ¹³C and ³¹P NMR study on the conformational properties of the branched tetramer U_{3'}p_{5'}A_{3'}p_{5'}^{2p5'G} (2) and compare them with that of the branched trimer A_{3'}p_{5'}^{2p5'G}U (1) (Figure 1). In this study, the ¹H-¹H, ¹H-³¹P and ¹³C-³¹P coupling constants of the branched tetramer 2 have been measured in order to obtain more detailed information about its backbone conformation which has not been hitherto reported in the literature.

Assignment of resonances. The assignment of the proton resonances for the branched trimer 1 has been reported elsewhere^{3d} and will not be discussed here. All the sugar protons and non exchangeable base protons in tetramer 2 could be assigned from the interpretation of several 2D NMR spectra. The resonances of the sugar protons of 2 were assigned using a COSY 45 experiment in which the second 90° pulse is replaced by a 45° pulse to achieve better resolution of the cross peaks close to the diagonal. To resolve some ambiguities in assignment due to overlap of absorptions in the H3', H4' and H5'/H5'' region, a homonuclear Hartmann-Hahn (HOHAHA) experiment was also performed (Figure 2). The adenosine residue was easily assigned by the characteristic downfield shift of its H2' and H3' protons. The H1' of adenosine is the most downfield signal of all anomeric protons. The 5'-terminal uridine residue was identified by the upfield shift of its H5'/H5'' protons and by the absence of their coupling with phosphorus. The two remaining sugars were assigned from the interpretation of the 2D ¹H-³¹P correlation spectrum (Figure 3). The 2'→5' phosphate is always the most shielded ³¹P signal and it experiences a spin-spin coupling with the H5'/H5'' of guanosine and H2'A. The assignment of the H-6 and H-5 of the pyrimidine moieties were based on their distinctive coupling constants: H-6 and H-5 of uridine appear as a doublet of ~ 8.1 Hz while H-6 and H-5 of cytidine appear as a doublet of ~ 7.6 Hz. The detailed assignments of the proton resonances are listed in Table 1. The carbon resonances for 1 and 2 were assigned using a proton-detected ¹H-¹³C chemical shift correlation experiment (Figure 4).

Table 1: Proton chemical shifts (ppm) of U_{3'}p_{5'}A_{3'}p_{5'}^{2p5'G} (2).

	T °C	1'	2'	3'	4'	5'	5''	H8	H2	H6	H5
Up	27 °C	5.67	4.07	4.30	3.99	3.59	3.51			7.55	5.72
	45 °C	5.68	4.09	4.32	3.99	3.59	3.50			7.49	5.70
pAp	27 °C	6.18	5.32	4.96	4.50	4.20	4.05	8.24	8.00		
	45 °C	6.17	5.29	4.92	4.50	4.17	4.04	8.25	8.02		
pG	27 °C	5.63	4.43	4.27	4.12	4.03	4.01	7.68			
	45 °C	5.61	4.38	4.19	4.05	3.92	3.92	7.71			
pC	27 °C	5.88	4.22	4.29	4.23	4.30	4.17			7.80	5.91
	45 °C	5.86	4.19	4.26	4.20	4.25	4.15			7.78	5.92

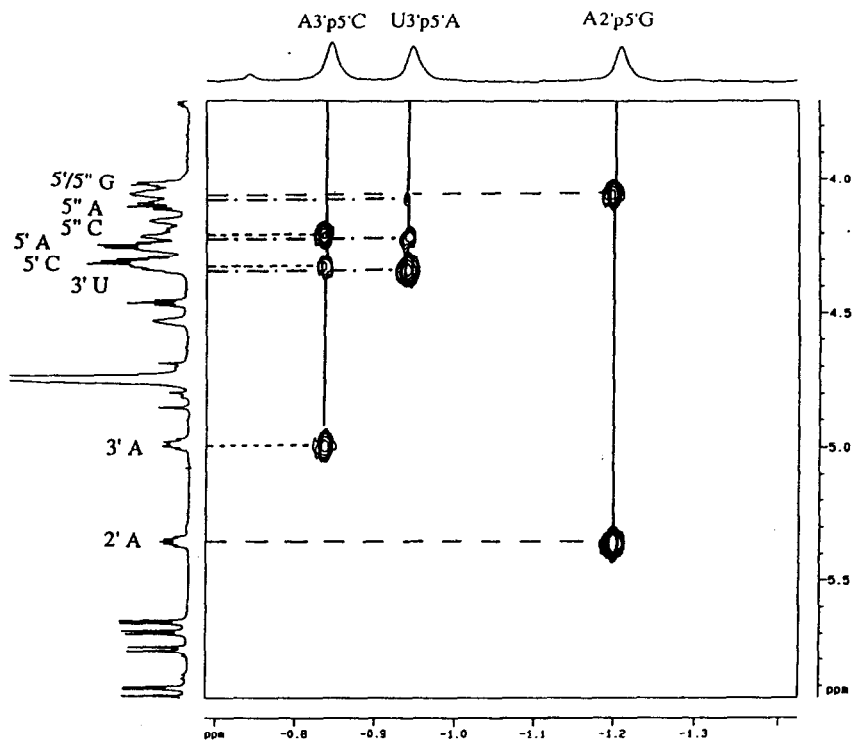


Figure 3: ^{31}P - ^1H chemical shifts correlation spectrum for 2 at 27 °C in D_2O . The 1D ^{31}P spectrum is shown on the top and the 1D ^1H spectrum on the left side of the 2D spectrum.

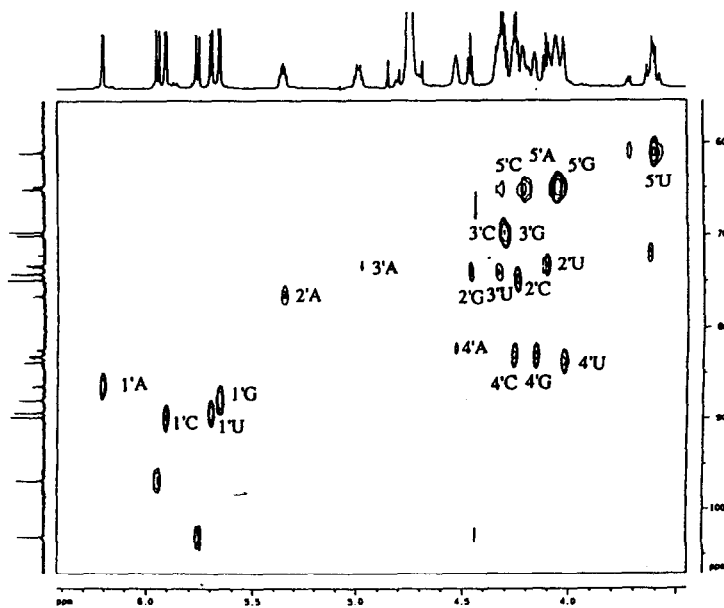


Figure 4: Proton detected ^{13}C - ^1H chemical shifts correlation spectrum for 2 at 27 °C in D_2O . Only the correlations between the anomeric protons and carbons are shown.

Conformational analysis. The ^1H - ^1H coupling constants for **1** and **2** were measured at two different temperatures (27 °C and 45 °C) from one dimensional spectra and from 2D J-resolved spectra with phosphorus decoupling. These coupling constants were further refined by spin-spin simulation and are listed in Tables 2 and 3.

Table 2: ^1H - ^1H and ^1H - ^{31}P coupling constants (Hz) for $\text{A}_{3'}^{2p5'}\text{G}_{3'p5'}\text{U}$ (1)

	T °C	1'2'	2'3'	3'4'	4'5'	4'5''	2'P2'	3'P3'	4'P5'	5'P5'	5''P5'
pAp	27 °C	5.9	4.8	3.2	2.4	2.9	8.6	7.9			
	45 °C	6.0	4.9	2.9	2.4	3.2	9.1	7.6			
pG	27 °C	4.9	4.9	4.9	2.4	2.9			1.5	4.4	3.9
	45 °C	5.2	5.2	4.7	2.9	3.4			1.8	5.0	3.9
pU	27 °C	4.9	5.4	4.1	2.4	3.0			1.5	5.0	4.4
	45 °C	4.9	5.4	4.4	2.7	3.3				5.2	4.4

A double quantum filtered (DQF) COSY spectrum with and without phosphorus decoupling (Figure 5) were also recorded to compare the coupling constants obtained by this method (1 Hz resolution) with those obtained from the J-resolved experiment (0.2 Hz resolution). The accuracy in the observed coupling constants by both of these techniques were comparable, and we have therefore subsequently used DQF COSY to obtain an estimation of ^1H - ^1H coupling in larger systems such as branched pentamer and heptamer⁷.

Table 3: ^1H - ^1H and ^1H - ^{31}P coupling constants (Hz) for $\text{U}_{3'p5'}\text{A}_{3'p5'}^{2p5'}\text{G}_{3'p5'}\text{C}$ (2)

	T °C	1'2'	2'3'	3'4'	4'5'	4'5''	2'P2'	3'P3'	4'P5'	5'P5'	5''P5'
Up	27 °C	5.4	5.4	4.1	3.0	4.0			a		
	45 °C	5.6	5.6	4.4	3.0	4.0			7.9		
pAp	27 °C	3.8	5.2	5.5	2.3	4.1	9.0	8.1	1.8	3.3	3.6
	45 °C	4.6	4.7	4.7	2.6	4.7	9.0	8.3	a	4.7	4.2
pG	27 °C	5.0	4.8	4.9	3.0	3.0			2.6	a	a
	45 °C	5.0	5.2	5.2	3.0	3.0			3.1	a	a
pC	27 °C	4.1	4.7	5.4	1.9	3.1			2.8	2.5	5.2
	45 °C	4.0	4.8	5.1	2.5	3.4			a	3.6	5.8

^a Could not be determined.

Conformation of the sugar ring. In aqueous solution, the sugar ring of a ribonucleotide is known to exist in an equilibrium of two rapidly interconverting conformers denoted by N (C3'-endo) and S (C2'-endo). The geometries of the N and S conformers expressed as their phase angle of pseudorotation (P_N and P_S) and their puckering amplitude (ϕ_N and ϕ_S) with their molar fractions, which can be deduced from the ^1H - ^1H coupling constants $J_{1'2'}$, $J_{2'3'}$ and $J_{3'4'}$ ⁸. In RNA, only three couplings are available and a full pseudorotational analysis requires the measurement of the coupling constants at different temperatures. Moreover, the overlap of sugar proton absorptions observed in RNA often makes an accurate determination of all coupling constants difficult. It

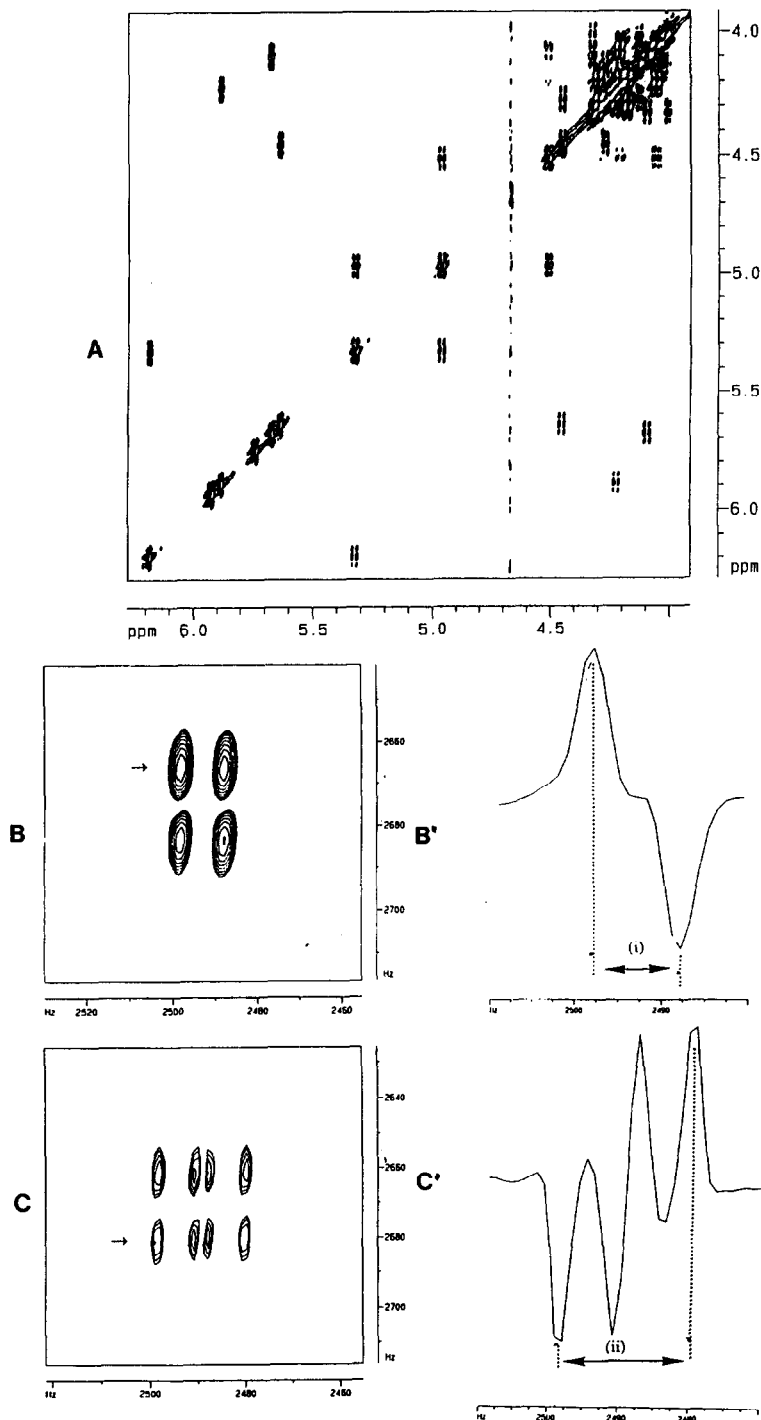


Figure 5. (A):DQF COSY, phosphorus decoupling, spectrum of **2** at 27 °C in D₂O. (B) and (C): Expansion of the adenosine 2'-3' cross peak in the ³¹P decoupled and ³¹P coupled DQF COSY. Vertical slices through these patterns taken at the site indicated by an arrow are shown in (B') and (C'). The arrow length (i) sums the $J_{1'2'}$ and $J_{2'3'}$. The difference in the total width of these spectra (subtraction of the arrow lengths (i) and (ii) provides an estimation of $3J_{HP}$

is however, possible to estimate the population of N type conformer from the $J_{1'2'}$ coupling constant using the equation 19:

$$\%N = 100 (J_{1'2'}^S - J_{1'2'}^{obs}) / (J_{1'2'}^S - J_{1'2'}^N) \quad \dots \quad (1)$$

when $J_{1'2'}^S$ and $J_{1'2'}^N$ being the coupling constants of the S and N conformers, respectively.

The pseudorotational parameters for **1** and **2** were calculated using the program PSEUROT¹⁰ and are listed in Table 4. The graphical representation of the N populations in Figure 6 shows a major difference in the behaviour between the adenosine residues in the trimer **1** and tetramer **2**. In trimer **1**, the sugar of adenosine prefers the S conformation (74 % at 27 °C) while in tetramer **2**, it prefers the N conformation (61% at 27° C). Upon an increase of temperature, the N \rightleftharpoons S equilibrium of the adenosine sugar in the trimer **1** is not affected.

In the tetramer **2**, the increase of temperature results in a decrease of the population of N conformer. This behaviour is similar to what is observed in 3'→5' oligoribonucleotides. In both the trimer **1** and tetramer **2**, the 2'→5' linked guanosine and the 3'→5' linked pyrimidine nucleotide do not show any clear preference for the N or S type conformation. In tetramer **2**, the sugar ring of the 5'-terminal uridine residue is oriented toward more S conformation (66 % at 27 °C). The change of conformation observed for the adenosine sugar from trimer **1** to tetramer **2** reflects a direct influence of the additional 5'-terminal uridine residue.

Conformation of the glycosidic bond. At 500 MHz, 2D NOESY and ROESY experiments (mixing times of 300 and 900 ms) did not give any information about the spatial proximities between nucleobases, and only intraresidual NOE connectivities could be observed. The absence of interresidual NOE is most probably due to the lack of rigidity of the molecule. The fact that some NOE between nucleobases could be observed at 270 MHz^{3b} for **2** suggest that the absence of NOE at 500 MHz could be instead due to the rotational correlation time τ_c . In the present work, no attempt has been made to calculate τ_c .

Table 4: Pseudorotational parameters P, ϕ and population of N type conformer

	$A_{3'p5'U}^{2p5'G}$ (1)			$U_{3'p5'A}^{2p5'G} A_{3'p5'C}$ (2)			
	pAp	pG	pU	Up	pAp	pG	pC
P_N	10°	0°	-15°	-16°	24°	15°	4°
ϕ_N	40°	38°	36°	38°	36°	40°	39°
P_S	162°	143°	149°	139°	173°	144°	159°
ϕ_S	38°	41°	37°	39°	39°	41°	38°
%N at 27 °C	26	44	41	34	61	40	55
%N at 45 °C	26	39	42	32	47	43	53

From 2D NOESY or ROESY experiments, the orientation of the base (*syn* or *anti*) relative to its sugar ring can be obtained. A nucleoside is considered to prefer an *anti* conformation when a strong NOE between its H8 (H6)

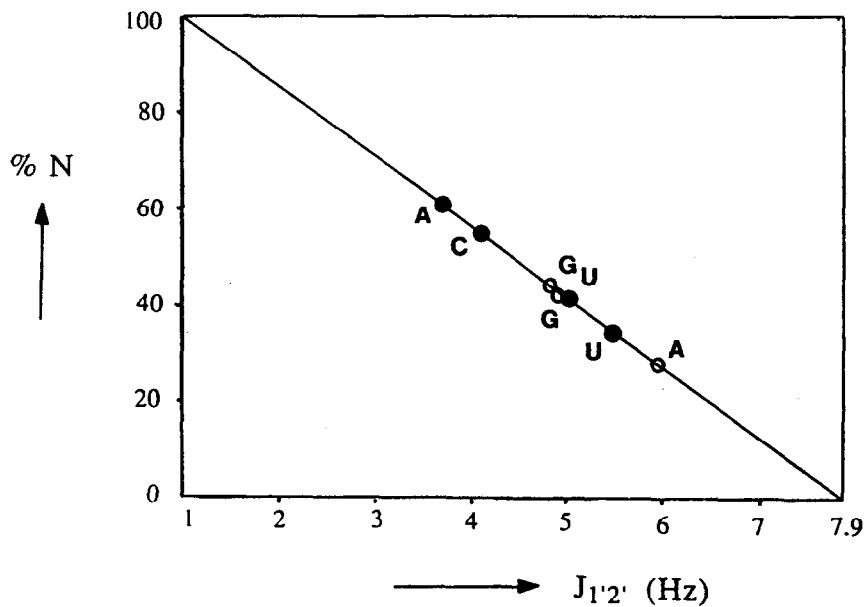


Figure 6: Graphical representation of the experimental $J_{1'2'}$ values and of the corresponding population of N conformer for the sugar rings of trimer 1 [○] and of tetramer 2 [●]

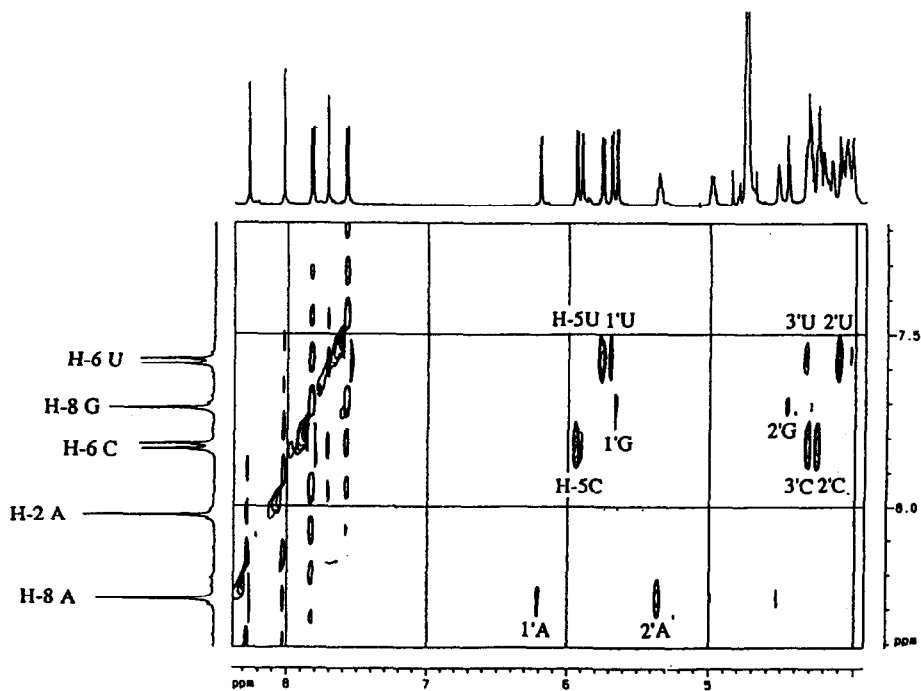


Figure 7: ROESY spectrum for **2** at 27 °C in D_2O . The intraresidual connectivities between the aromatic (left side of the spectrum) and the anomeric protons (top of the spectrum) are shown. Mixing time of 300 ms.

and its H2' together with a weak NOE between its H8 (H6) and its H1' proton is observed. A *syn* conformation is preferred when a stronger NOE between the H8 (H6) and its H1' proton is observed. In **1**, the H8 of adenosine shows a strong NOE with its H1' suggesting a *syn* conformation. The H8 of guanosine and H6 of uridine on the other hand show stronger NOE with their respective H2' and H2' / H3' which suggest an *anti* conformation for guanosine and uridine in the trimer **1** (not shown). In **2** (Figure 7), the two pyrimidine residues are in *anti* conformation (NOE between H6 and H2' and H3'). The guanosine is in *syn* conformation (Stronger NOE between H8 and H1'). The H8 of the adenosine branch point shows a weak NOE with its H1' and a stronger NOE with its H2' suggesting an *anti* conformation. It should be noted that the combination of *S* and *syn* conformation observed for the adenosine in **1** is not commonly encountered in oligoribonucleotides¹¹ as found from X-ray crystallographic studies.

Backbone conformation. To establish the conformation of the phosphate backbone, the ¹³C-³¹P coupling constants and the ¹H-³¹P coupling constants have been determined for **1** and **2**. The ¹³C-³¹P coupling (Tables 5 & 6) were measured from the one dimensional carbon NMR spectra with proton decoupling.

Table 5 : ³¹P-¹³C coupling constants (Hz) of A₃p^{5'}G (1) .

	T °C	C1'P2'	C2'P2'	C2'P3'	C3'P2'	C3'P3'	C4'P3'	C4'P5'
pAp	27 °C	7.6	5.6	6.6	3.0	5.1	<1Hz	
	45 °C	7.2	5.5	6.7	4.2	4.8	<1Hz	
pG	27 °C							9.7
	45 °C							8.6
pU	27 °C							8.6
	45 °C							8.2

The ¹H-³¹P coupling constants were measured from 2D J-resolved spectra. The F2 axis of the 2D spectrum contains both homonuclear (¹H-¹H) and heteronuclear (¹H-³¹P) coupling informations. After a tilt, the F2 axis loses the ¹H-¹H coupling information but retains the ¹H-³¹P couplings. Thus, in the projection of the F2 domain, a proton coupled with a phosphorus appears as a doublet. Information about the ¹H-³¹P coupling constants were also obtained from the comparison of the 1D NMR proton spectra with and without phosphorus decoupling.

Conformation about the C4'-C5' bond (γ). The conformational behaviour about the C4'-C5' bond is monitored by means of the vicinal ¹H-¹H coupling J_{4'5'} and J_{4'5''}. The population of the γ^+ rotamer can be calculated using the sum rule equation: 2¹²:

$$\% \gamma^+ = 100 (13.3 - (J_{4'5'} + J_{4'5''})) / 9.7 \quad \dots \quad (2)$$

The data in Table 7 show that γ^+ of all residues are highly populated. In the trimer **1** however, an increase of temperature has more effect on the γ^+ population of the 2'→5' linked guanosine than on the 3'→5' linked

uridine. For the guanosine residue, the γ^+ population changes from 82% at 27 °C to 71% at 45 °C while it changes from 81% at 27 °C to 77% at 45 °C for the uridine residue. In the tetramer 2 the effect of temperature

Table 6: ^{31}P - ^{13}C coupling constants (Hz) for 2.

	T°C	C1'P2'	C2'P2'	C2'P3'	C3'P2'	C3'P3'	C4'P3'	C4'P5'
Up	27 °C			4.6		5.1	3.6	
	45 °C			4.8		5.2	4.0	
pAp	27 °C	2.8	5.1	4.6	5.6	4.6	2.0	9.3
	45 °C	4.8	5.6	5.2	5.2	5.2	2.5	8.6
pG	27 °C							8.3
	45 °C							8.0
pC	27 °C							8.8
	45 °C							8.4

increase on the population of γ^+ rotamer is greater for the 3'→5' linked cytidine and the adenosine branch-point than for the 2'→5' linked guanosine. The γ^+ population for the adenosine residue changes from 71% at 27 °C to 62% at 45 °C and for the cytidine residue it changes from 85% at 27 °C to 76% at 45 °C. The guanosine nucleotide has an invariant 76% of γ^+ population at 27 °C and 45 °C. The decrease of γ^+ populations observed when the temperature is increased can be attributed to a destacking of the molecule along the A2'→5'G nucleotides in the trimer 1, and along the U3'→5'A3'→5'C nucleotides in the tetramer 2.

Conformation about C5'-O5' (β). The rotamer population about the C5'-O5' bond can be monitored by the ^1H - ^{31}P and ^{13}C - ^{31}P coupling constants: $J_{\text{H5}^{\prime}\text{P5}^{\prime}}$, $J_{\text{H5}^{\prime}\text{P5}^{\prime}}$ and $J_{\text{C4}^{\prime}\text{P5}^{\prime}}$. The population of the preferred *trans* conformer (β^t) can be estimated independently from the J_{HP} and J_{CP} couplings using the equations^{4,13}:

$$\% \beta^t = (25.5 - (J_{\text{H5}^{\prime}\text{P5}^{\prime}} + J_{\text{H5}^{\prime}\text{P5}^{\prime}})) / 20.5 \quad \dots \quad (3)$$

$$\% \beta^t = (J_{\text{C4}^{\prime}\text{P5}^{\prime}} - 0.73) / 10.27 \quad \dots \quad (4)$$

Table 8 shows the population of β^t rotamer for 1 and 2 calculated both from the ^1H - ^{31}P and from the ^{13}C - ^{31}P coupling constants. The *trans* rotamer is highly populated for all residues. This preference for the *trans* conformation is a general feature for stacked oligoribonucleotides. In the trimer 1, the *trans* rotamer is slightly more populated for the guanosine than for the uridine nucleotide. On the other hand, in the tetramer 2 the temperature increase has less effect on the β^t torsion of 2'-guanosine residue compared to those of adenosine and 3'-cytidine residues. As it is seen that the decrease of β^t populations upon temperature-increase also follows the same trend as the γ^+ population (*vide supra*), which together can be attributed to a destacking of the tetramer 2 molecule along the U3'→5'A3'→5'C nucleotides while the trimer 1 destacks along the A2'→5'G nucleotides.

Conformation about C3'-O3' (ϵ) and C2'-O2' (ϵ'). In 3'→5' linked oligoribonucleotides, the ϵ^+ rotamer does not appear¹⁴ and only the ϵ^- and ϵ^t rotamers need to be considered. Similarly, the existence of ϵ^+ conformer in the 2'→5' linked oligoribonucleotides is unlikely. The conformation about the C3'-O3' and C2'-O2' bonds

were therefore analyzed in terms of a three-state equilibrium between ϵ^- , ϵ^+ ; ϵ^- , ϵ^+ and ϵ^t , ϵ^+ . The ϵ^t , ϵ^+ conformation can probably be excluded for steric reasons and electrostatic repulsions between the two phosphate groups⁴.

Table 7: Population of *gauche*⁺ rotamer about C4'-C5' (γ^+)

	A ₃ ^{2'p5'G} / ₃ ^{p5'U}			U ₃ ^{2'p5'G} / ₃ ^{p5'C}			
	pAp	pG	pU	Up	pAp	pG	pC
% γ^+ [27 °C]	82	82	81	65	71	76	85
% γ^+ [45 °C]	79	71	77	65	62	76	76

The preferred conformation about the C3'-O3' bond can be estimated from the $J_{C_2'P_3'}$, $J_{C_4'P_3'}$ and $J_{H_3'P_3'}$ coupling constants. The expected magnitude of $J_{C_4'P_3'}$ and $J_{C_2'P_3'}$ for a pure ϵ^- conformation is 0.5 Hz and 9.4 Hz ($\epsilon = 275^\circ$) and for a pure ϵ^+ conformation; they are 7.4 Hz and 1.4 Hz respectively ($\epsilon = 219^\circ$). In the trimer **1**, the small $J_{C_4'P_3'}$ (< 1 Hz) and large $J_{C_2'P_3'}$ (6.7 Hz) coupling constants observed for the adenosine nucleotide at 27° C indicate a high population of *gauche*⁻ conformer about the C3'-O3' bond. In the tetramer **2**, the values of $J_{C_2'P_3'}$ (4.6 Hz) and $J_{C_4'P_3'}$ (3.6 Hz) measured for the 5'-terminal uridine residue suggest that the C3'-O3' bond is equally populated with ϵ^- and ϵ^+ rotamers. The small $J_{C_4'P_3'}$ (2.0 Hz) for the adenosine residue is an indication of a preferred ϵ^- conformation about the C3'-O3' bond. The analysis of $J_{C_1'P_2'}$ and $J_{C_3'P_2'}$ yields information on the conformation about the C2'-O2' bond. A large $J_{C_1'P_2'}$ and a small $J_{C_3'P_2'}$ indicate a high population of ϵ^- conformer. In compound **1**, the large $J_{C_1'P_2'}$ (7.6 Hz) and smaller $J_{C_3'P_2'}$ (3.0 Hz) couplings measured for the adenosine nucleotide suggest a preference for the ϵ^- conformation about the C2'-O2' bond. In the tetramer **2**, the small value of the $C_1'P_2'$ coupling constant (2.8 Hz) at 27 °C is an indication that the C2'-O2' bond is mainly in a ϵ^+ conformation. Upon an increase of temperature, the value of $J_{C_1'P_2'}$ increases to 4.8 Hz. This could be interpreted as a decrease of the population of ϵ^+ rotamer. We however can not explain why $J_{C_3'P_2'}$ is so little affected by temperature increase.

Table 8: Population of *trans* rotamer about C5'-O5' (β^t)

	A ₃ ^{2'p5'G} / ₃ ^{p5'U}		U ₃ ^{2'p5'G} / ₃ ^{p5'C}		
	pG	pU	pAp	pG	pC
% β^t [27 °C]	84 ^a	78 ^a	90 ^a	/	87 ^a
	87 ^b	76 ^b	83 ^b	73 ^b	78 ^b
% β^t [45 °C]	80 ^a	77 ^a	80 ^a	/	78 ^a
	76 ^b	73 ^b	76 ^b	71 ^b	74 ^b

^a Calculated using equation 3.

^b Calculated using equation 4.

For 3'→5' linked ribonucleotides or deoxyribonucleotides, it has been shown that the sugar ring puckering equilibrium is related to the conformation of the C3'-O3' bond¹⁵: the C3'-O3' bond preferentially adopts an ϵ^t conformation for a sugar ring in the N conformation and an ϵ^- conformation for the sugar ring in the S conformation. In tetramer 2, the adenosine branch-point shows an exceptional behaviour owing to the observation that its C3'-O3' adopts an ϵ^- for a sugar ring with the N conformation. It is likely that an additional 2'→5' phosphate and the overall stacking properties of the molecule forces the branch-point adenosine in the unusual combination of conformations of ϵ^- and N.

Conclusion: Our present 500 MHz NMR study of the trimer 1 and tetramer 2 has provided new informations about the conformational properties of the backbone for the core $A_{3'}^{2p5G}$ of the branched RNA structures. In the trimer 1, the sugar ring of the adenosine branch point adopts more of the S-type conformation and the conformation about the glycosidic bond is *syn*. The C3'-O3' and C2'-O2' bonds are both in a *gauche* conformation. The overall conformation of the molecule is dominated by an A2'→5'G stacking. In the tetramer 2, the sugar ring of the adenosine branch point adopts preferentially the N-type conformation and the glycosidic bond is in the *anti* conformation. The C3'-O3' and C2'-O2' bonds are in *gauche* and *trans* conformations respectively. The A3'→5'C interaction is preferred over a A2'→5'G stacking. These results are in agreement with previous studies from this laboratory^{3,6} where temperature induced chemical shifts changes and NOE connectivities were used to monitor the stacking behaviour. It was concluded from these studies that natural branched trimers stack along the 2'→5' nucleotides, while branched tetramers stack along the 3'→5' axis. 2D NOESY experiments at 270 MHz showed the following important weak NOEs: AH8 with UH6, AH2 with CH6, CH6 with GH8, and UH6 with GH8. The NOEs seen between AH8 with UH6, and AH2 with CH6 show that the tetramer 2 stacks along the U3'→5'A3'→5'C nucleotides (Model A, Fig. 8). This is now clearly substantiated by the present observation that branch-point A and 3'-terminal C residues show a pronounced decrease of γ^t and β^t populations upon temperature-increase, which is attributed to a destacking along the U3'→5'A3'→5'C axis. It may be noted that γ^t and β^t populations of 2'→5'-linked guanosine nucleotide is rather insensitive to temperature-change. On the other hand, the NOEs seen between CH6 with GH8, and UH6 with GH8 suggest spatial proximities between 5'-terminal U and 2'-terminal G, and 3'-terminal C with 2'-terminal G residues (Model B, Fig. 8).

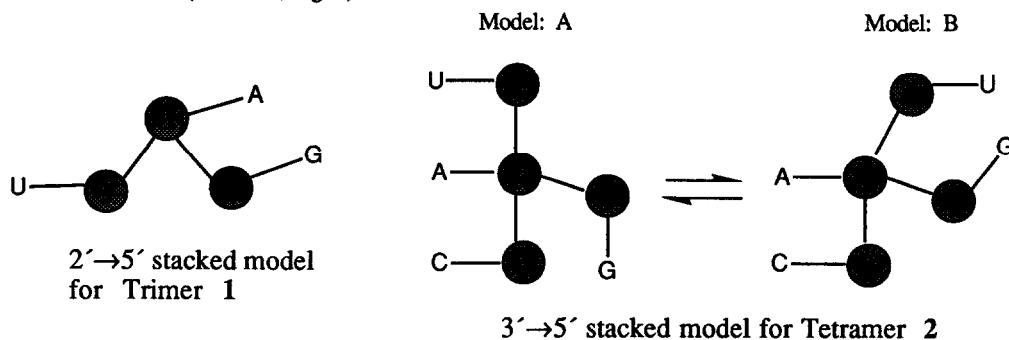


Figure 8

The introduction of a 5'-terminal uridine residue shifts the molecular conformation from an A2'→5'G stack in the trimer 1 to a A3'→5'C stack in the tetramer 2. This is a new example of 5'-conformational transmission which has been also noticed in some linear trimeric, tetrameric and pentameric RNA^{16,17}.

Experimental

NMR sample preparations: The NMR samples were lyophilized twice from 99.8% D₂O. The samples were then dissolved in 0.5 ml of 99.96 % D₂O and transferred into 5 mm tubes. A trace of dry acetonitrile was added as an internal reference for chemical shift measurements. The sample concentration was 3 mM for 1 and 5 mM for 2. **NMR acquisitions:** All NMR spectra were recorded on a Bruker AMX-500 spectrometer. ¹H-NMR spectra were collected with 32K data points and zero filled to 64K data points. The 1D proton spectra were simulated using the DAISY simulation program supplied by Bruker.

2D COSY spectra were recorded using the COSY 45 pulse sequence for enhanced resolution of the cross peaks near the diagonal. The data were collected in the absolute magnitude mode with 2K data points in the F2 direction and 512 points in the F1 direction. The matrix were zero-filled to 2K x 2K data points and a sine bell function was applied in both domains before Fourier transformation. 2D DQF COSY¹⁸ with and without phosphorus decoupling were recorded in the phase sensitive mode. The data were collected with 4K data points in the F2 direction and 512 points in the F1 direction. For a sweep width of 4000 Hz, a resolution of 1.1 Hz was achieved in the F2 direction. A sine square bell window was applied before Fourier transformation. 2D HOHAHA, NOESY and ROESY spectra were recorded in phase sensitive mode with time proportional phase incrementation (TPPI) with presaturation of the water peak. For the HOHAHA experiment, a mixing time of 150 ms was used, 256 Fids consisting of 1K data points were zero-filled to 2K x 2K data points and a sine square bell multiplication was applied in both directions before Fourier transformation. The NOESY and ROESY¹⁹ experiment was performed at two different mixing time (900 ms and 300 ms). 256 FIDs consisting of 1K points were zero-filled to 1K x 1K data points. A sine bell multiplication was applied before Fourier transformation. 2D J-resolved experiments, with and without phosphorus decoupling, were performed using 64 FIDs consisting of 4K data points and zero-filled to 8k x 128 data points. A sine square bell multiplication was applied in the F1 direction and a sine bell multiplication was applied in the F2 direction before Fourier transformation. The ¹H-³¹P chemical shift correlation experiment²⁰ was performed in the absolute magnitude mode. The spectral range used was 600 Hz in the F2 direction and 3000 Hz in the F1 direction. A 1K x 256 data set was zero filled to 1K x 1K data points and a sine square bell multiplication was applied in both directions before Fourier transformation. The proton detected ¹³C-¹H chemical shift correlation experiment²¹ was performed in the phase sensitive mode. 1K x 256 data points were zero-filled to 1K x 1K data points. A sine square bell function was applied in both directions before Fourier transformation.

Acknowledgements

Authors thank Swedish Board for Technical Development and Swedish Natural Science Research Council. for generous financial supports. Authors also thank Wallenbergs Stiftelsen, University of Uppsala and Swedish Research Council (FRN) for funds toward the purchase of 500 MHz NMR spectrometer. Financial support

from the European Molecular Biology Organization (EMBO) through a two-year EMBO fellowship to L.H.K is gratefully acknowledged.

References

1. (a) T. R. Cech and B. L. Bass, *Ann. Rev. Biochem.*, **55**, 599 (1986); (b) P. A. Sharp, *Science*, **235**, 766 (1987); (c) M. M. Konarska, P. J. Grabowski, R. A. Padgett and P. A. Sharp, *Nature* (London), **313**, 552 (1985); (d) B. Ruskin and M. R. Green, *Science*, **229**, 135 (1985).
2. (a) H. Horning, M. Aebi and C. Weissman, *Nature*, **324**, 589 (1986); (b) M. Aebi, H. Horning, R. A. Padgett, J. Reiser and C. Weissmann, *Cell*, **47**, 555 (1986).
3. (a) G. Remaud, J-M. Vial, A. Nyilas, N. Balgobin and J. Chattopadhyaya, *Tetrahedron*, **43**, 947 (1987); (b) J-M. Vial, G. Remaud, N. Balgobin and J. Chattopadhyaya, *Tetrahedron*, **43**, 3997 (1987); (c) G. Remaud, N. Balgobin, A. Sandström, J-M. Vial, L. H. Koole, H. M. Buck, A. F. Drake, X-X. Zhou and J. Chattopadhyaya, *J. Biochem. Biophys. Meth.*, **18**, 1 (1989); (1989); (d) L. H. Koole, N. Balgobin, H. M. Buck, W. H. A. Kuipers, A. Nyilas, G. Remaud, J-M. Vial and J. Chattopadhyaya, *Recl. Trav. Chim. Pays-Bas*, **107**, 663 (1988).
4. M. J. Damha and K. K. Olgivie, *Biochemistry*, **27**, 6403 (1988).
5. M. Lee, S. Huss, G. Gosselin, J-L. Imbach, J. A. Hartley and J. W. Lown, *J. Biomol. Struct. Dyn.*, **5**, 651 (1987).
6. (a) X-X. Zhou, A. Nyilas, G. Remaud and J. Chattopadhyaya, *Tetrahedron*, **44**, 571 (1988); (b) G. Remaud, N. Balgobin, C. Glemarec and J. Chattopadhyaya, *Tetrahedron*, **45**, 1537 (1989); (c) A. Sandström, G. Remaud, J-M. Vial, X-X. Zhou, A. Nyilas, N. Balgobin and J. Chattopadhyaya, *J. Chem. Soc., Chem. Commun.*, 542 (1988).
7. L.H. Koole, P. Agback, C. Glemarec, X-X. Zhou, and J. Chattopadhyaya, (in preparation)
8. (a) C. Altona and M. Sundaralingam, *J. Am. Chem. Soc.*, **94**, 8205 (1972); (b) C. Altona and M. Sundaralingam, *J. Am. Chem. Soc.*, **95**, 2333 (1973).
9. (a) J. Doornbos, C. T. J. Wreemann, J. H. van Boom and C. Altona, *Eur. J. Biochem.*, **131**, 571 (1983); (b) F. A. A. M. de Leeuw and C. Altona, *J. Chem. Soc. Perkin II*, **375** (1982).
10. (a) F. A. A. M. de Leeuw and C. Altona, *J. Comp. Chem.*, **4**, 428 (1983); (b) F. A. A. M. De Leeuw and C. Altona, *Quant. Chem. Progr. Exch.*, 463, University of Indiana at Bloomington. (1983).
11. H. P. M. de Leeuw, C. A. G. Haasnoot and C. Altona, *Isr. J. Chem.*, **20**, 108 (1980).
12. C. Altona, *Recl. Trav. Chim. Pays-Bas*, **101**, 413 (1982).
13. P. P. Lankhorst, C. A. G. Haasnoot, C. Erkelens and C. Altona, *J. Biomol. Struct. Dyn.*, **1**, 1387 (1984).
14. (a) M. Sundaralingam, *Biopolymers*, **7**, 821 (1969); (b) C. Altona, J. H. van Boom, J. R. de Jager, H. J. Koeners and G. van Binst, *Nature* (London), **247**, 558 (1974); (c) J. L. Aldefer and P. O. P. Ts' o, *Biochemistry*, **16**, 2410 (1977).
15. D. B. Davies and H. Sadikot, *Biopolymers*, **22**, 1843 (1983)
16. Y. Th. van den Hoogen, S. J. Treurniet, H. C. P. F. Roelen, E. de Vroom, G. A. van der Marel, J. H. van Boom and C. Altona, *Eur. J. Biochem.*, **171**, 155 (1988).
17. M. P. Stone, D. L. Johnson and P. N. Borer, *Biochemistry*, **20**, 3604 (1981).
18. Neuhaus, D., Wagner, G., Vasak, M., Kägi, J.H.R., Wuthrich, K., *Eur. J. Biochem.*, **151**, 257 (1985).
19. A. Bax and D. G. Davies, *J. Magn. Reson.*, **63**, 207 (1985).
20. A. Bax and G. A. Morris, *J. Magn. Reson.*, **42**, 501 (1981).
21. A. Bax, R. H. Griffey and B. L. Hawkins, *J. Magn. Reson.*, **55**, 301 (1983).